Fish and Shellfish Immunology 120 (2022) 620–632

Contents lists available at ScienceDirect

Fish and Shellfish Immunology

journal homepage: www.elsevier.com/locate/fsi

A novel ferritin L (FerL) in hybrid crucian carp could participate in host defense against *Aeromonas hydrophila* infection and diminish inflammatory signals

Ning-Xia Xiong [a], Jie Ou [a], Shi-Yun Li [a], Jia-Hui Zhao [b], Jin-Fang Huang [a], Ke-Xin Li [a], Sheng-Wei Luo [a,*], Shao-Jun Liu [a,**], Ming Wen [a], Chang Wu [a], Shi Wang [a], Kai-Kun Luo [a], Fang-Zhou Hu [a], Qing-Feng Liu [a]

[a] State Key Laboratory of Developmental Biology of Freshwater Fish, College of Life Science, Hunan Normal University, Changsha, 410081, PR China
[b] Foreign Studies College, Hunan Normal University, Changsha, 410081, PR China

ARTICLE INFO

Keywords:
Crucian carp
Ferritin L
Gene expression
Aeromonas hydrophila

ABSTRACT

FerL, a multifunctional iron-storage polypeptide, not only exhibited a regulatory role in iron metabolism, but also participated in the regulation of fish immunity. In this study, ORF sequence of WR-FerL was 522 bp, encoding 173 amino acid residues. Tissue-specific analysis revealed that the highest expression of WR-FerL was detected in spleen. *A. hydrophila* challenge and LPS stimulation could sharply enhance WR-FerL mRNA expression in tissues and fish cells, respectively. Purified WR-FerL fusion peptide exhibited *in vitro* binding activity to *A. hydrophila* and endotoxin, limited bacterial dissemination to tissues as well as attenuated *A. hydrophila*-induced production of pro-inflammatory cytokines. Moreover, WR-FerL overexpression could abrogate NF-κB and TNFα promoter activity in fish cells. These results indicated that WR-FerL could play an important role in host defense against *A. hydrophila* infection.

1. Introduction

Exposure to ambient stressors may cause occurrences of severe diseases in mammals [1]. Broadly speaking, biotic or abiotic stressors may disrupt physiological function [2] and suppress immune response in fish [3]. Iron metabolism participates in a variety of biological processes, including synthesis of various enzymes [4], regulation of innate immunity [5], occurrence of metabolic diseases [6] and growth performance [7], whereas excessive level of intracellular iron level can elicit an adverse effect on organisms, including reactive oxygen species (ROS) accumulation, antioxidant imbalance and destruction of macromolecular cell products, finally leading to tissue damage and cell malfunction [8]. Previous studies demonstrate that mammalian ferritin, an iron storage protein, is detected in all cell types of the body as multiple isoferritins composed of 24 subunits of ferritin H (FerH) and ferritin L (FerL) [9]. In contrast, FerH and ferritin M (FerM) are the predominant ferritin subunits in fish, while the evidence for the existence of FerL in fish is scanty [10]. As known iron-regulatory proteins, hepcidin is firstly discovered as a iron regulatory hormone peptide regulated by immune-related signals in mammals [11–13], which can serve as antimicrobial peptides participating in both iron metabolism and immune defense against bacterial infection in fish [14–18]. Recent studies demonstrate that ferritin deletion may increase induced levels of hepcidin and cause abnormal iron absorption regulated by hepcidin alone, suggesting that ferritin may play an important role in both iron homeostasis and antimicrobial peptide metabolism [19]. In addition, ferritin can also serve as one of important indicators or acute phase proteins (APPs) during pathogenic stimulation or malignancies occurrence [20–22].

In general, fish possess various forms of pathogen-recognizing properties, developed complement cascades as well as immune-related signals [23,24]. Although mammalian ferritin has been extensively studied, some reports only focus on the characterization of FerH and FerM in fish [25–28]. Recent studies firstly discover the existence of L subunit in seahorse, whose transcript levels can be up-regulated following bacterial stimulation [29]. However, the data on

* Corresponding author.
** Corresponding author.
E-mail addresses: swluo@hunnu.edu.cn (S.-W. Luo), lsj@hunnu.edu.cn (S.-J. Liu).

https://doi.org/10.1016/j.fsi.2021.12.040
Received 23 July 2021; Received in revised form 12 November 2021; Accepted 23 December 2021
Available online 27 December 2021

immunomodulatory role of FerL in fish is limited.

Crucian carp (*Carassius auratus*) is one of the most important economic freshwater fish and abundant in lakes, rivers and reservoirs in China, which is popular with fish farmers [30]. Currently, white crucian carp (*Carassius cuvieri*, WCC) and red crucian carp (*Carassius auratus* red var, RCC) are classified into different species in the genus of *Carassius* [31], thus generation of hybrid crucian carp (WR) by crossing of WCC (2n = 100, ♀) and RCC (2n = 100, ♂) is considered as interspecific hybridization [32]. Apart from documented problems, the aquaculture of crucian carp is ravaged by environmental deterioration, which may render fish less resistant to pathogenic infection [33,34]. Additionally, the emergence of global climate change may exhibit a lingering effect in the expansion of water-borne pathogenic diseases, posing a great threat to the survival of aquatic animals [35]. Previous studies demonstrate that *A. hydrophila* challenge can significantly increase accumulative mortality of allogynogenetic crucian carp [36]. Thus, this study on the immune response to gram-negative bacterial infection in crucian carp may be propitious to the sustainable development of aquaculture.

In this study, the aims were to characterize architecture of WR-FerL in hybrid crucian carp and measure tissue distribution of WR-FerL mRNA. We also assessed the effect of bacterial infection on the expression patterns of WR-FerL mRNA in various immune tissues. To further characterize its function, we also studied binding activity of WR-FerL to *A. hydrophila* and its potential effect on bacterial growth *in vitro* and *in vivo*, which may provide a new insight to the immune regulation of FerL in crucian carp.

2. Materials and methods

2.1. Animals

Hybrid crucian carp (WR) was generated by crossing white crucian carp (*Carassius cuvieri*, WCC, ♀) and red crucian carp (*Carassius auratus* red var, RCC, ♂) [37]. Healthy WRs with approximately 23.50 ± 0.79 g were obtained from an aquaculture base in Wang Cheng district (Changsha, Hunan province, China).WRs were acclimatized with the diluted freshwater for two weeks and fed with commercial diet twice daily till 24 h before challenge experiment.

2.2. Cell culture

Hybrid crucian carp fin cells (WRFCs) were cultured at 26 °C with a humidified atmosphere of 5% CO_2 as described in our previous studies [38].

2.3. Gene cloning and bioinformatics analysis

According to cloning protocols, ORF sequence of WR-FerL was obtained as previously described [39]. Gene-specific primers were shown in Table 1. Domain structure and phylogenetic analysis of predicted WR-FerL amino acid sequence were constructed by using NCBI blast, ExPASy tools, SignalP 5.0 server, PredictProtein server, Phyre2 system and MEGA 6.0, respectively.

2.4. Immune challenge with A. hydrophila

A. hydrophila preparation and immune challenge experiment were based on our previous studies [40]. In brief, 100 μl suspension of 1×10^7 CFU ml^{-1} *A. hydrophila* in PBS was injected intraperitoneally, while injection of 100 μl sterile PBS was used as the control group [41]. Each group was composed of six individuals and each treatment contained three replicates under the same condition. Tissues were isolated at 0, 6, 12, 24, 36 and 48 h post-injection, immediately frozen in liquid nitrogen and preserved in −80 °C.

Table 1
The primer sequences used in this study.

Primer names	Sequence direction (5' → 3')	Use
FerL-F	ATGTCTCTAGTCAAGCAGAA	clone
FerL-R	TCAGAGCGTGTGCTTGTCAAA	clone
pET-FerL-F	CCGGAATTCATGTCTCTAGTCAAGCAGAA	vector
pET-FerL–R	CCGCTCGAGTTAATGATGATGATGATGATGGAGCGTGTGCTTGTCAAACA	vector
pc-FerL-F	CCCAAGCTTGCATGTCTCTAGTCAAGCAGAA	vector
pc-FerL-R	CCGGAATTCTTACTTGTCGTCATCGTCTTTGTAGTCGAGCGTGTGCTTGTCAAACAG	vector
RT-18S-F	CCGACCCTCCCTCACG	qPCR
RT-18S-R	GCCTGCTGCCTTCCTTG	qPCR
RT- FerL-F	CAGACCGTTGCGAAGCCC	qPCR
RT- FerL-R	GCCAGCGTAGTCACCCAGC	qPCR
RT-MyD88-F	CTATGAGGCGATTCCAGTAACA	qPCR
RT- MyD88-R	CCAGTCTGCTGCCACCG	qPCR
RT-IRAK4-F	GCGTCCTGCTGCCTGAT	qPCR
RT- IRAK4-R	CCTCTGAACACGATGCCAA	qPCR
RT-TRAF6-F	AGACCAGCAAGGCTATGACG	qPCR
RT- TRAF6-R	GCCGAGCGAAGACCCA	qPCR
RT-IL-1beta-1-F	CCTGACAGTGCTGGCTTTG	qPCR
RT- IL-1beta-1-R	AATGATGATGTTCACCACCTTC	qPCR
RT-IL-1beta-2-F	TCTTCGCATCCTCACAGCAT	qPCR
RT-IL-1beta-2-R	CAGCGTCACAGCCTTCAAAT	qPCR
RT-TNFalpha-1-F	GGATTGCTGCCCTCACGG	qPCR
RT-TNFalpha-1-R	CTTTGGACACTTTAGGTTCATACG	qPCR
RT-TNFalpha-2-F	GTGGGGTCCTGCTGGCT	qPCR
RT-TNFalpha-2-R	CTGGTCCTGGTTCTGTTTC	qPCR
RT-hlyA-F	GGCCGGTGGCCCGAAGATACGGG	qPCR
RT-hlyA-R	GGCGGCGCCGGACGAGACGGGG	qPCR
RT-GAPDH-F	CAGGGTGGTGCCAAGCG	qPCR
RT-GAPDH-R	GGGGAGCCAAGCAGTTAGTG	qPCR
RT-Bax-F	GGTGGAGGCGATACGGG	qPCR
RT-Bax-R	CGAGTTGGTTGAAGAGTGGAGT	qPCR
RT-caspase-3-F	AGATGCTGCTGAGGTCGGG	qPCR
RT-caspase-3-R	GGTCACCACGGGCAACTG	qPCR
RT-caspase-8-F	TGTGAATCTTCCAAAGGCAAA	qPCR
RT-caspase-8-R	CTGTATCCGCAACAACCGAG	qPCR

2.5. Fish cells treated with various doses of Lipopolysaccharide (LPS)

WRFCs were seeded in 6-well plates at 80% confluence for 24 h. After that, cell culture medium was replaced with fresh medium containing 500 ng/ml or 1000 ng/ml of LPS (*Escherichia coli* O111:B4, Sigma, USA) [42]. Cells were harvested at 0, 6, 12, 24, 36 and 48 h post-treatment, immediately frozen in liquid nitrogen and preserved in −80 °C.

2.6. RNA isolation, cDNA synthesis and qRT-PCR assay

Total RNA was extracted from isolated tissues and harvested cell samples by using HiPure Total RNA Mini Kit (Magen, China). Following quality check, 1000 ng of purified total RNA was used for cDNA synthesis by using Revert AidTM M-MuLV Reverse Transcriptase Kit (MBI Fermentas, USA). Then, expression profiles of WR-FerL were investigated by qRT-PCR assay [43]. In brief, qRT-PCR assay was performed by using PowerUp SYBR Green Master Mix (Applied Biosystems, USA). At the end of qRT-PCR assay, melting curve analysis was implemented to confirm credibility of each qRT-PCR result. The primers used in this study were shown in Table 1. 18S rRNA (XR_003291850.1) was used as internal control to normalize the results [44]. Primer specificity was confirmed and each sample was analyzed in triplicate to certify the repetitiveness and credibility of experimental results. qRT-PCR results were measured by using Applied Biosystems QuantStudio 5 Real-Time PCR System with $2^{-\triangle\triangle Ct}$ methods [45].

2.7. Plasmid preparation

To investigate WR-FerL function, ORF sequence of WR-FerL was used as the template. Following double digestion reaction, the above sequence was ligated to pET32a or pcDNA3.1 plasmids, which was subjected to the sequencing confirmation as previously described [46].

2.8. Prokaryotic expression, purification and western blotting of WR-FerL

The protocols of fusion protein expression and purification were performed as previously described [47]. In brief, the above pET32a plasmid or pET32a-WR-FerL plasmid was transformed into *E. coli* Rossetta (DE3) competent cells for protein expression, respectively. Rossetta clone inserted with a corrected plasmid was cultured in LB medium with 100 μg/ml ampicillin at 37 °C until OD_{600} value reached about 0.6, then IPTG was added to a final concentration of 1 mM for another 4 h induction. After IPTG induction and sonication, pellets were harvested, dissolved in the buffer containing 8 M urea and centrifuged, then the soluble recombinant proteins were obtained and purified by using Ni-NTA resins (Novagen, China). Following proper dialysis, the protein concentration and western blotting were performed. According to our previous studies, purified pET-32a tag peptide was kept in lab and used as the control [48].

2.9. Iron binding assay

The iron binding assay was performed as previously described [49]. In brief, various concentrations of purified pET32a tag or WR-FerL were co-cultured with 2 mM $FeCl_2$ at room temperature for 10 min. After that, 30 μl of 5 mM ferrozine was added to the solution. Following 15 min incubation at room temperature, the absorbance at 562 nm was measured by using a spectrophotometer. The experiment was performed in triplicate.

2.10. ELISA assay

Based on ELISA coating protocols [50], 96-well plates were coated with resuspension of *A. hydrophila* (1×10^7 CFU ml^{-1}) or LPS (100 μg/ml, purified from *Escherichia coli* O111:B4, Sigma, USA) at 4 °C overnight, then blocked with 5% milk and washed with 0.5% Tween-20/PBS. After that, various concentrations of purified pET32a tag or WR-FerL were added to the plates for 2 h incubation at room temperature, followed by incubation with anti-His antibody and HRP secondary antibody. Then, 200 μl of TMB diluted in substrate buffer was added and incubated for 30 min in dark. Until the color was developed, the reaction was stopped by adding.

2 M H_2SO_4. The absorbance at 450 nm was determined by a microplate reader. pET32a tag group was served as the control. The experiment was performed in triplicate. The binding index was calculated.

2.11. In vivo effect of WR-FerL on A. hydrophila infection

To investigate the effect of WR-FerL on growth of *A. hydrophila*, *in vivo* injection was performed. Thirty minutes after bacterial infection (1×10^7 CFU ml^{-1}), WRs received intraperitoneal injection of purified pET32a tag or WR-FerL at a dose of 3.0 μg/g, respectively. Following 24 h post-injection, both bacterial load assay and detection of *A. hydrophila* hlyA gene were performed as described previously [51]. In brief, bacterial loads were quantitated in liver, kidney and spleen. The tissues (approximately 0.15 g fresh tissue weight) were homogenized in 1.0 ml of sterile PBS and cultured onto LB agar plates for 16 h incubation, then bacterial colonies were counted [52]. For detection of *A. hydrophila* hlyA gene, both genomic DNA of tissues and bacterial DNA were extracted by using a DNA extraction kit (Omega, USA), and the concentration was adjusted to 100 ng/μl qPCR assay was used to detect hlyA gene of *A. hydrophila*, while GAPDH gene was analyzed as the reference gene. pET32a tag-treated group was used as the control. The experiments were performed in triplicate.

2.12. Protective effect of WR-FerL in the immune challenge with A. hydrophila

To investigate the effect of WR-FerL in *A. hydrophila* stimulated inflammatory response, the above pET32a tag or WR-FerL treated samples were used for RNA isolation and cDNA synthesis. Then, qRT-PCR assay was performed as described above. pET32a tag treated group was used as the control. The primers of myeloid differentiation factor 88 (MyD88, KC816578.1), interleukin-1 receptor-associated kinase 4 (IRAK4, XM_026202045.1), tumor necrosis factor receptor associated factor 6 (TRAF6, KF767099.1), interleukin-1β-1 (IL-1β-1, KC306642.1), interleukin-1β-2 (IL-1β-2, KC771268.1), tumor necrosis factor α-1 (TNFα-1, KJ923252.1), tumor necrosis factor α-2 (TNFα-2, KJ923253.1) and 18S rRNA were shown in Table .1. Each sample was analyzed in triplicate to certify the repetitiveness and credibility of experimental results. qRT-PCR results were measured by using QuantStudio 5 Real-Time PCR system (Applied Biosystems, USA) with $2^{-\triangle\triangle Ct}$ methods.

2.13. Dual-luciferase reporter assay

Based on previous studies, dual-luciferase reporter assay was performed in fish cells [53]. In brief, cells were grown in 24-well plates for 18 h. Cells were co-transfected with PRL-TK and NF-κB Luc/TNFα Luc [54]. Various amounts of recombinant vectors pcDNA3.1 or pcDNA3.1-WR-FerL were transfected to investigate transcriptional activity of reporter activities. To investigate the effect of LPS stimulation on promoter activities, transfected cells were stimulated with LPS at 100 ng/ml for 6 h [55]. Following 24 h, luciferase activity was performed by using a dual-luciferase reporter assay system (Promega). Relative folds of luciferase activity were normalized to the amount of Renilla luciferase. The results were repeated in triplicate.

2.14. Statistical analyses

The data analysis was measured by using SPSS 18 analysis program and represented as means ± standard deviation. All of the experimental data analysis was subjected to Student's *t*-test or one-way ANOVA (one-

way analysis of variance). In the further analysis of Duncan's multiple range test, only if the level of P-value < 0.05, the differences were considered statistically significant.

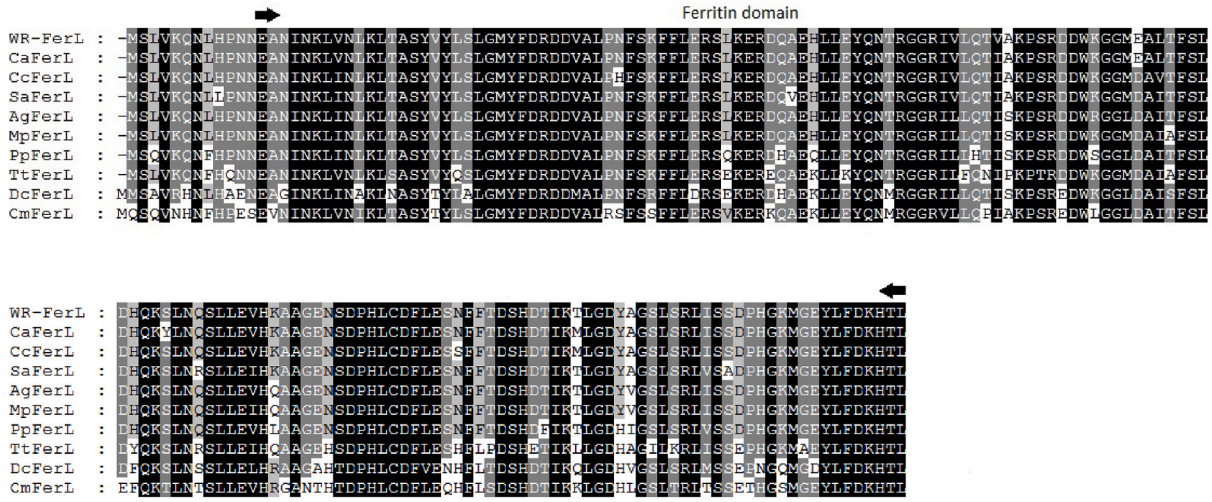

Fig.1A

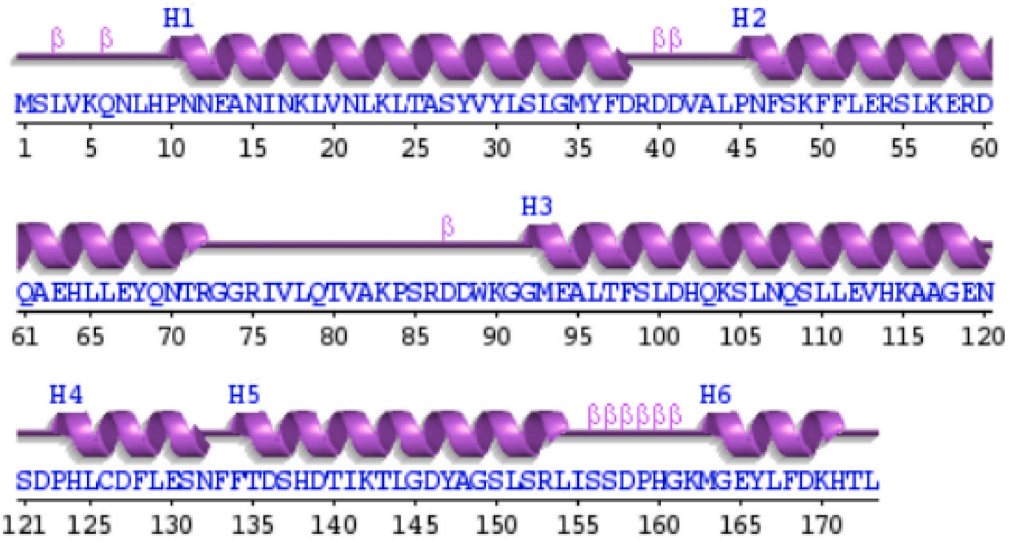

Fig.1B

Fig. 1. Bioinformatics analysis of WR-FerL. (A) Multiple alignment of the predicted amino acid sequence of WR-FerL with other FerL sequences. AgFerL, Anabarilius grahami Ferritin L, ROL51056.1; CaFerL, *Carassius auratus* Ferritin L, XP_026093571.1; CcFerL, *Cyprinus carpio* Ferritin L, XP_018922143.1; DcFerL, *Denticeps clupeoides* Ferritin L, XP_028845021.1; MpFerL, *Mylopharyngodon piceus* Ferritin L, AVO65126.1; OmFerL, *Oncorhynchus mykiss* Ferritin L, XP_021420938.2; PpFerL, *Pimephales promelas* Ferritin L, XP_039522540.1; SaFerL, *Sinocyclocheilus anshuiensis* Ferritin L, XP_016310750.1; TtFerL, *Triplophysa tibetana* Ferritin L, KAA0704991.1. The shared residues represented the similar regions between the different species and the conservative degree was distinguished from light to dark. Ferritin-like domain was indicated by arrow. (B) Secondary structure of WR-FerL was predicted by PDBsum Generate. : Helix strand; Helices labeled: H1, H2, …and strands by their sheets A, B, …; β: beta turn. (C) 3D structure of WR-FerL was predicted by using Phyre2. Tertiary structure of WR-FerL was colored by rainbow from N to C terminus. 100% of residues were modeled at >90% confidence Model dimensions (Å): X:44.914, Y:46.296, Z:57.031. (D) Phylogenetic tree constructed by using full-length amino acid sequences of FerL. Full-length FerL amino acid sequences were extracted from Genbank and analyzed by using Neighbor-Joining method by Mega 6.0 with 1000 bootstrap replications. The numbers shown at branches indicated the bootstrap values (%). Sequence used in analysis with their latin names and GenBank accession number: *Labrus bergylta* FerL, XP_020496361.1; *Stegastes partitus* FerL, XP_008281518.1; *Betta splendens* FerL, XP_028989547.1; *Channa argus* FerL, KAF3704483.1; *Epinephelus lanceolatus* FerL, XP_033466545.1; *Trematomus bernacchii* FerL, XP_034006194.1; *Cyprinodon tularosa* FerL, XP_038156978.1; *Oncorhynchus mykiss* FerL, XP_021420938.2; *Denticeps clupeoides* FerL, XP_028845021.1; *Triplophysa tibetana* FerL, KAA0704991.1; *Carassius auratus* FerL, XP_026093571.1; *Cyprinus carpio* FerL, XP_018922143.1; *Sinocyclocheilus anshuiensis* FerL, XP_016310750.1; *Mylopharyngodon piceus* FerL, AVO65126.1; *Anabarilius grahami* FerL, ROL51056.1; *Pimephales promelas* FerL, XP_039522540.1; *Xenopus laevis* FerL, AAQ10929.1; *Podarcis muralis* FerL, XP_028559083.1; *Homo sapiens* FerL, NP_000137.2.

Fig.1C

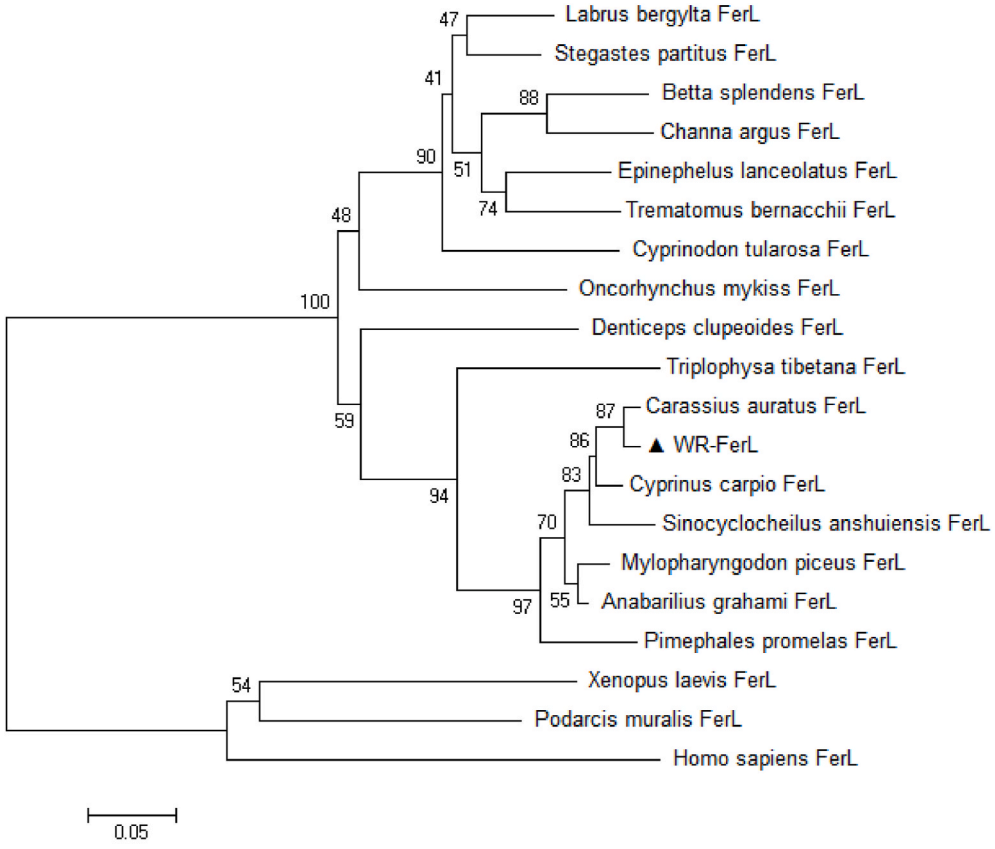

Fig.1D

Fig. 1. (*continued*).

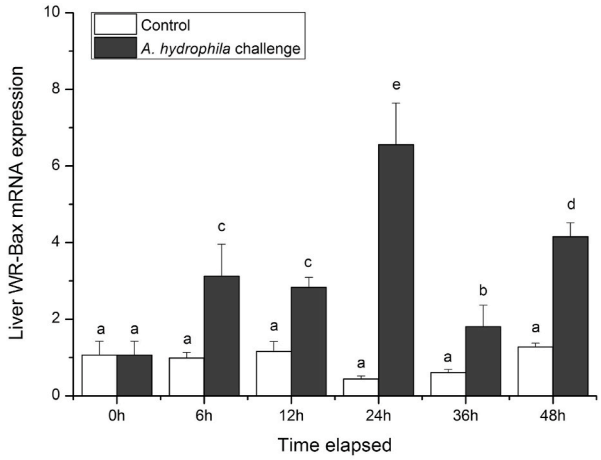

Fig.2A

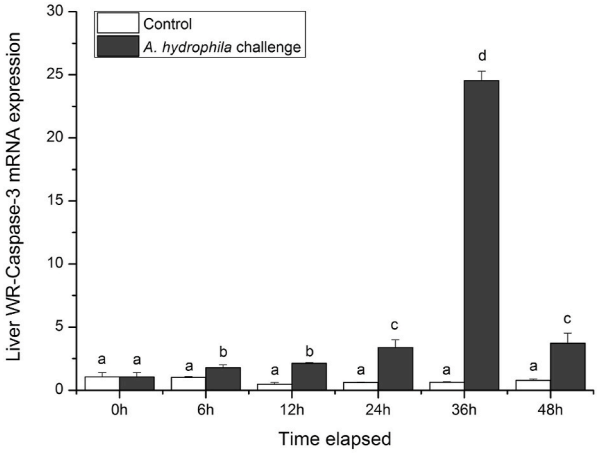

Fig.2D

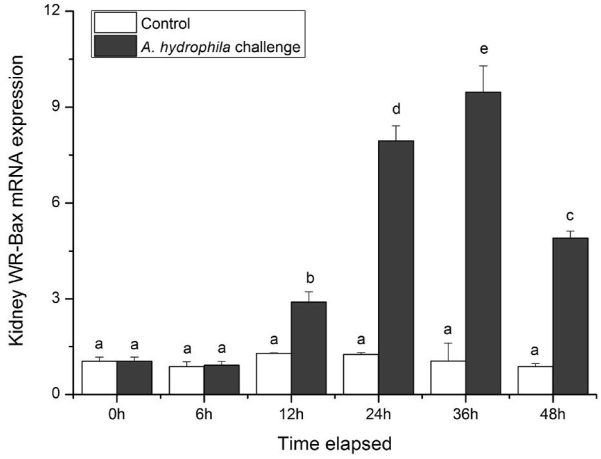

Fig.2B

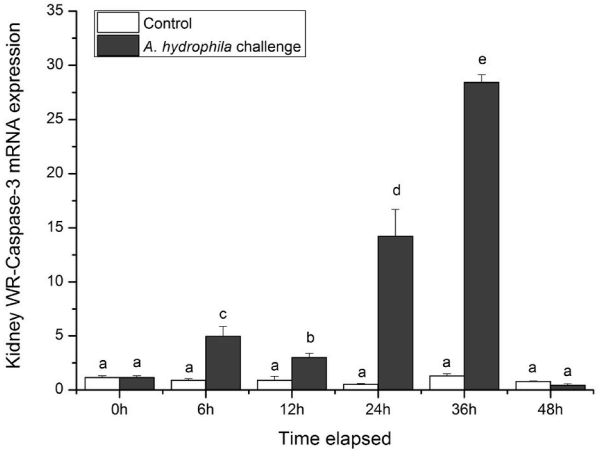

Fig.2E

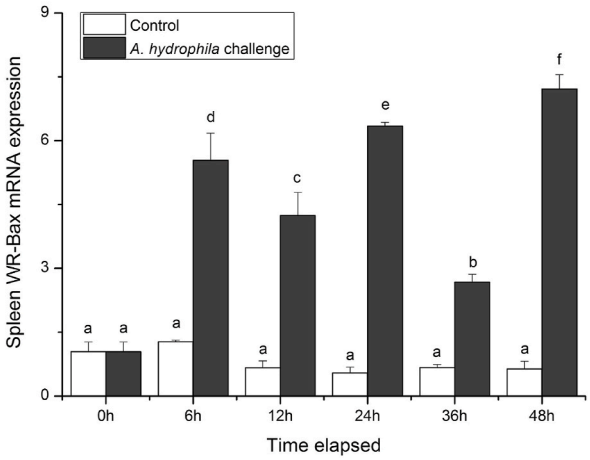

Fig.2C

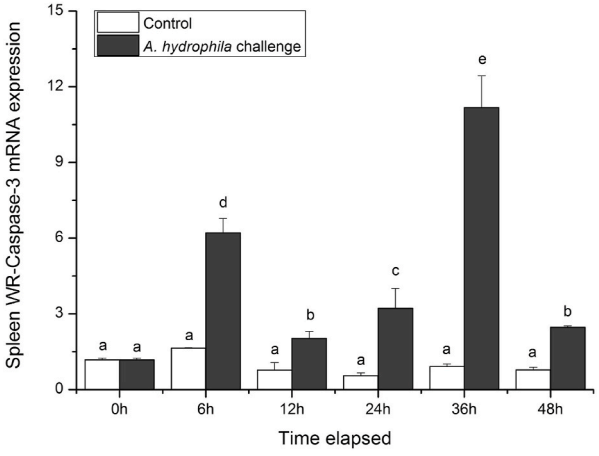

Fig.2F

Fig. 2. Expression profiles of apoptosis-related genes determined by qRT-PCR. The calculated data (mean ± SD) of six individuals (n = 6) with different letters were significantly different ($P < 0.05$).

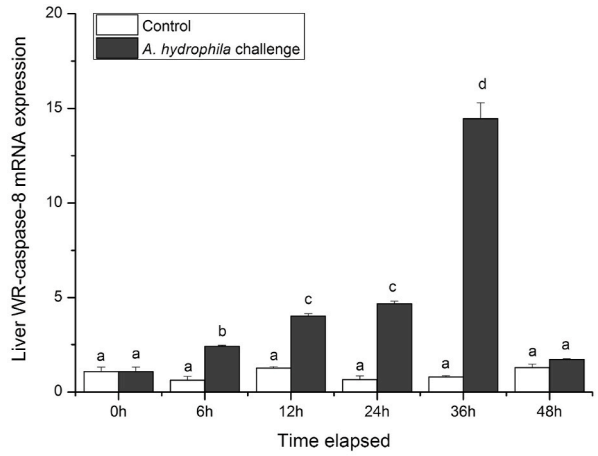

Fig.2G

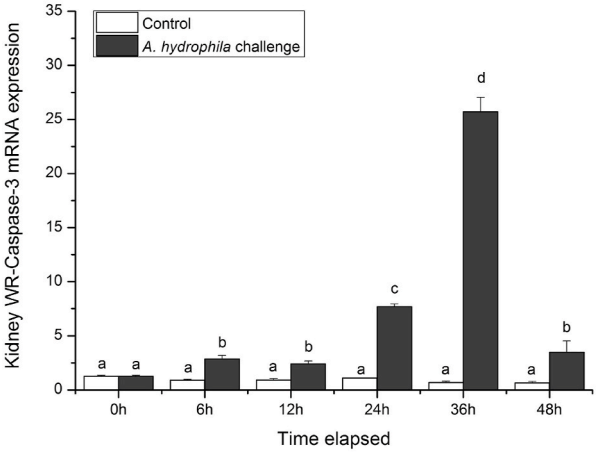

Fig.2H

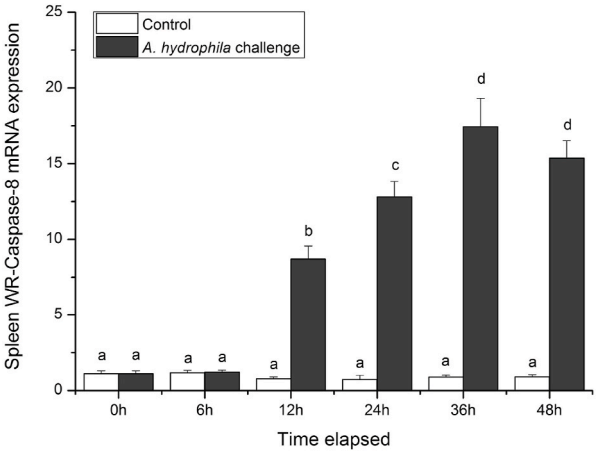

Fig.2I

Fig. 2. (*continued*).

3. Results

3.1. Characterization of WR-FerL sequence

The obtained ORF sequence of WR-FerL was 522 bp, encoding 173 amino acid residues with an estimated molecular mass of 19.66 KDa and a predicted isoeletric point of 6.13. In Fig. 1A, multiple sequence alignment analysis revealed that WR-FerL contained a ferritin-like domain (13–153 amino acid), showing a high similarity to the counterparts in other vertebrates. Additionally, NCBI blast system discovered that WR-FerL polypeptide harbored the conserved ferroxidase diiron center (K^{23}, Y^{30}, K^{57}, E^{58}, Q^{61}, Q^{103} and S^{137}), ferrihydrite nucleation center (E^{53},L^{56}, K^{57} and D^{60}) and iron ion channel (H^{114}, D^{127} and E^{130}). In Fig. 1B, secondary structure analysis predicted that WR-FerL contained 6 helices, 13 helix-helix interactions and 11β-turns. In Fig. 1C, tertiary structure of WR-FerL was 50% identical to d1mfra template modeled with 100% of residues exceeding a 90% confidence. In Fig. 1D, phylogenetic tree analysis revealed that WR-FerL sequence was similar to those of other teleost, suggesting that the evolutionary relationship was in agreement with the concept of the traditional taxonomy.

3.2. A. hydrophila challenge promote activation of apoptosis-related genes

In Fig. 2, expression profiles of apoptosis-related genes (Bax, caspase-3 and caspase-8) in liver, kidney and spleen were investigated following *A. hydrophila* challenge. In Fig. 2A, liver WR-Bax mRNA expression peaked at 24 h after *A. hydrophila* challenge. In Fig. 2B, a gradual increase of WR-Bax mRNA expression in kidney was observed from 12 h to 36 h following *A. hydrophila* challenge, followed by a sharp decrease at 48 h. In Fig. 2C, splenic WR-Bax mRNA expression dramatically fluctuated and peaked at 48 h after *A. hydrophila* challenge. In Fig. 2D-F, WR-caspase-3 mRNA in liver, kidney and spleen increased significantly from 6 h to 36 h following *A. hydrophila* challenge, followed by a sharp decrease at 48 h. In Fig. 2G-I, WRs receiving *A. hydrophila* infection exhibited a gradual increase of WR-caspase-8 mRNA expression from 6 h to 36 h.

3.3. Gene expression of WR-FerL mRNA

In Fig.3A, a high-level expression of WR-FerL mRNA was observed in spleen, while the lowest expression level was detected in muscle. Expression patterns of WR-FerL mRNA in liver, kidney and spleen were investigated at 0, 6, 12, 24, 36 and 48 h following *A. hydrophila* challenge. In Fig. 3B, liver WR-FerL mRNA expression peaked at 6 h following *A. hydrophila* challenge, followed by a sharp decrease from 12 h to 48 h. In Fig. 3C, a significant increase of WR-FerL mRNA expression in kidney was observed from 6 h to 48 h after *A. hydrophila* challenge with the highest value peaked at 36 h. In Fig. 3D, WR-FerL mRNA expression in spleen increased dramatically from 6 h to 12 h following *A. hydrophila* challenge, followed by a dramatic decrease from 24 h to 48 h.

Expression profiles of WR-FerL mRNA in WRFCs were investigated at 0, 6, 12, 24, 36 and 48 h after various doses of LPS stimulation. In Fig. 3E, expression levels of WR-FerL mRNA in WRFCs increased gradually and peaked at 36 h following 500 ng/ml LPS stimulation. In contrast, WR-FerL mRNA expression increase dramatically from 6 h to 24 h following 1000 ng/ml LPS stimulation, followed by a sharp decrease from 36 h to 48 h (Fig. 3F).

3.4. Prokaryotic expression and fusion protein validation

The pET32a and pET32a-WR-FerL plasmid were transformed into *E. coli* Rossetta (DE3) competent cells for protein expression, respectively. After IPTG induction, whole cell lysates were detected by SDS-PAGE. In. Fig.4A, a strong protein band was visualized in pET32a-WR-FerL transformed cells compared with that of pET32a transformed cells. Following sonication, WR-FerL fusion protein was purified by using a Ni-NTA resin (Millipore) and confirmed by western blotting using anti-His antibody.

3.5. Iron depriving activity of WR-FerL

To investigate the fundamental property of WR-FerL polypeptide harboring conserved metal binding sites, iron depriving assay was performed. As shown in Fig. 4B, the relative iron binding activity decreased significantly in high dose of WR-FerL compared with that of pET32a tag group, suggesting that fusion WR-FerL possessed an iron binding activity *in vitro*.

3.6. Binding activity of WR-FerL to A. hydrophila and LPS

In Fig.5A and 5B, recombinant WR-FerL exhibited a gradual increase of *in vitro* binding ability to *A. hydrophila* and LPS by comparing with those of the control, implying that WR-FerL could directly bind to *A. hydrophila* and LPS *in vitro*.

3.7. Antibacterial activity of WR-FerL against A. hydrophila

In Fig. 6A-B, bacterial load and detection of *A. hydrophila* hlyA in liver, kidney and spleen tissue were determined at 24 h post-infection. In this study, the administration of fusion WR-FerL could sharply reduce the bacterial loads in tissues. In addition, the expressions of *A. hydrophila* hlyA in liver, kidney and spleen in *A. hydrophila* + WR-FerL group were approximately 71.1%, 97.6% and 86.9% lower than those of *A. hydrophila* + pET32α tag group, respectively. These results suggested that the administration of WR-FerL could restrict growth of *A. hydrophila in vitro* and reduce its dissemination to tissues *in vivo*.

3.8. Regulatory effect of WR-FerL in A. hydrophila-induced inflammatory response

To investigate the immunoregulatory effect of WR-FerL in *A. hydrophila* -induced cytokine cascades, expression levels of MyD88, IRAK4, TRAF6, IL-1β-1, IL-1β-2, TNFα-1 and TNFα-2 were detected at 24 h post-challenge.

As shown in Fig. 7A-G, liver expression levels of MyD88, IRAK4, TRAF6, IL-1β-1, IL-1β-2, TNFα-1 and TNFα-2 mRNA in *A. hydrophila* + WR-FerL group were approximately 70.5%, 63.1%, 82.1%, 82.3%, 38.2%, 75.2% and 69.1% lower than those of *A. hydrophila* + pET32a tag group, respectively. In kidney, expressions of MyD88, IRAK4, TRAF6, IL-1β-1, IL-1β-2, TNFα-1 and TNFα-2 mRNA in *A. hydrophila* + WR-FerL group were approximately 98.0%, 97.1%, 97.6%, 64.7%, 85.0%, 98.7% and 94.8% lower than those of *A. hydrophila* + pET32a tag group, respectively. In addition, expressions of splenic MyD88, IRAK4, TRAF6, IL-1β-1, IL-1β-2, TNFα-1 and TNFα-2 mRNA in *A. hydrophila* + WR-FerL group were 93.2%, 88.7%, 94.0%, 84.0%, 38.2%, 67.2% and 42.1% lower than those of *A. hydrophila* + pET32a tag group, respectively.

3.9. WR-FerL overexpression suppressed NF-κB and TNFα activation in WRFCs

To detect the effect of WR-FerL overexpression on NF-κB and TNFα promoter activity, dual-luciferase assay was performed. As shown in Fig. 8A, WR-FerL overexpression could dramatically abrogate NF-κB luciferase reporter in WRFCs. 500 ng WR-FerL plasmid could attenuate NF-κB luciferase activity to 56.2%, while 1000 ng WR-FerL plasmid could decrease NF-κB activity to 44.7%. In addition, NF-κB reporter activity induced by LPS stimulation could be inhibited by 500 ng WR-FerL plasmid to 56.6%, while 1000 ng WR-FerL plasmid could mitigate increased level of NF-κB activity to approximately 40.3%.

In Fig. 8B, WR-FerL overexpression could significantly attenuate

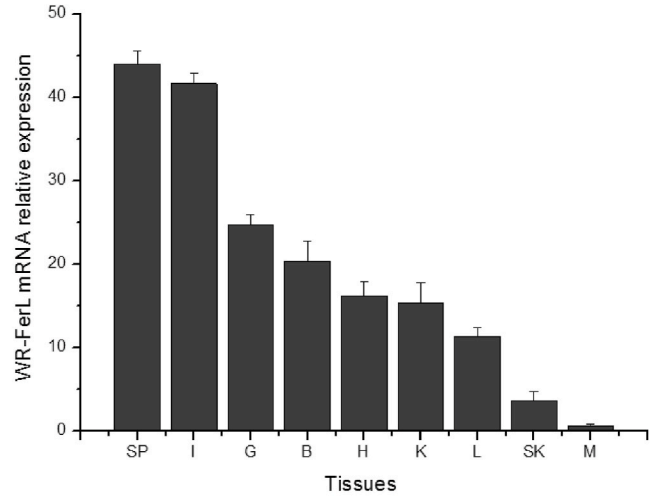

Fig.3A

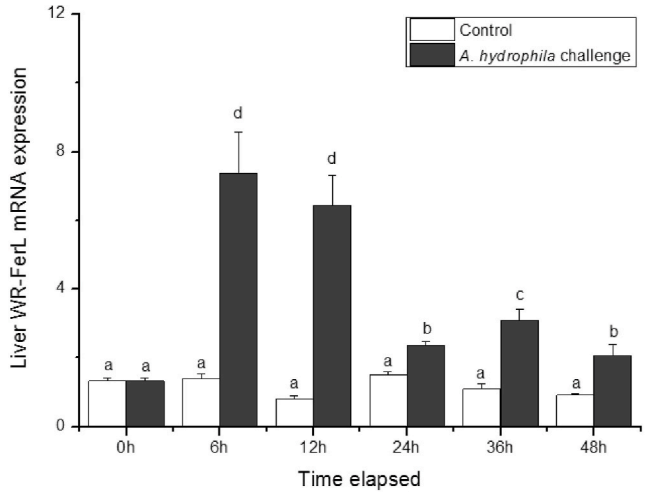

Fig.3B

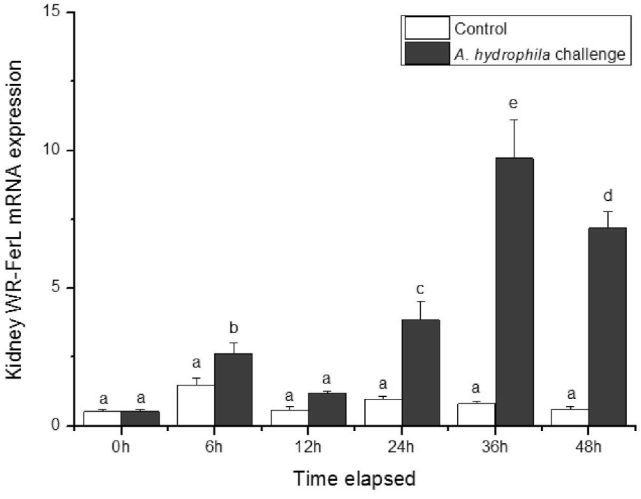

Fig.3C

(caption on next column)

Fig. 3. Gene expression of WR-FerL determined by qRT-PCR. (A) Tissue-specific mRNA expression of WR-FerL determined by qRT-PCR. Relative WR-FerL mRNA expression of each tissue was calculated by the $2^{-\triangle\triangle Ct}$ methods using 18S rRNA as a reference gene, and the relative mRNA level was compared with spleen expression. (L: liver; I: intestine; K: kidney; H: heart; SK: skin; G: gill; M: muscle; B: brain; SP: spleen). (B–D) qRT-PCR analysis of WR-FerL mRNA expression in liver, kidney and spleen at 0, 6, 12, 24, 36 and 48 h post-challenge. (E–F) qRT-PCR analysis of WR-FerL mRNA expression in WRFCs at 0, 6, 12, 24, 36 and 48 h following various doses of LPS stimulation. The calculated data (mean ± SD) of six individuals (n = 6) with different letters were significantly different ($P < 0.05$).

TNFα promoter activity in WRF cells. 500 ng WR-FerL plasmid could attenuate TNFα activity to approximately 64.2%, while 1000 ng WR-FerL plasmid could reduce TNFα activity to 33.3%. In addition, TNFα reporter activity induced by LPS stimulation could be inhibited by 500 ng WR-FerL plasmid to 59.9%, while 1000 ng WR-FerL plasmid could alleviate increased level of TNFα activity to approximately 25.9%.

4. Discussion

Previous studies have indicated that ROS overproduction induced by stressors may play a regulatory role in signal transduction for bridging innate immunity with adaptive immune response [56], whereas its long-term increase can disrupt antioxidant balance and damage macromolecular products [57]. Our previous studies suggested that LPS-induced inflammation and mitochondrial damage may be highly associated with ROS-mediated cytotoxic stress [54]. In general, apoptosis or programmed cell death (PCD) is highly modulated cell death process in the normal development and homeostasis within the host that can promote resolution of the acute inflammatory response and remodel inflamed sites via phagocytic clearance of dying cells [58,59]. Bax, a pro-apoptotic member of Bcl-2 like superfamily, can be activated in a p53-dependent manner by various stimuli [60]. In addition, Bax is required for the activation of caspase-8 and caspse-3 during apoptotic process [61], which is widely considered as a major determinant in p53-Bax apoptotic signals [62]. In this studies, increased levels of Bax, caspase-8 and caspase-3 expression were observed in liver, kidney and spleen following *A. hydrophila* challenge, suggesting that the activation of apoptosis-related genes can serve as the indicators of fish following *A. hydrophila* infection.

FerL is a ubiquitous iron storage protein of ferritin-like superfamily. Increasing evidences indicate that mammalian FerL can participate in occurrences of autoimmune disease [63] and confer protection against sepsis-induced inflammatory response [64]. However, the studies on existence of FerL in fish and its function of immune regulation are sparse. Current study revealed that the obtained WR-FerL sequence of 522 bp encoded 173 amino acid residues, possessing the ferritin-like domain, ferroxidase diiron center, ferrihydrite nucleation center and iron ion channel. In this study, we found that WR-FerL exhibited the ferroxidase activity. Similarly, previous studies have shown that the presence of partially conserved residues of ferroxidase centers in seahorse FerL may exhibit an observed ferroxidase activity [29].

Tissue-specific analysis revealed that a high-level of WR-FerL expression was observed in spleen, while the lowest expression level was detected in muscle, suggesting that the expression of WR-FerL mRNA was broadly expressed in various tissues. In general, liver, kidney and spleen play vital roles in fish immunity [65]. In this study, elevated expression levels of WR-FerL mRNA were detected in liver, kidney and spleen after *A. hydrophila* challenge. In addition, WRFCs receiving various doses of LPS stimulation exhibited a significant up-regulated expression of WR-FerL mRNA. These results implied that WR-FerL may be involved in immune response to *A. hydrophila* infection and gram-negative bacterial endotoxin stimulation. However, the potential function of FerL in fish is still scanty.

Iron metabolism is not only critical for the growth of microorganisms

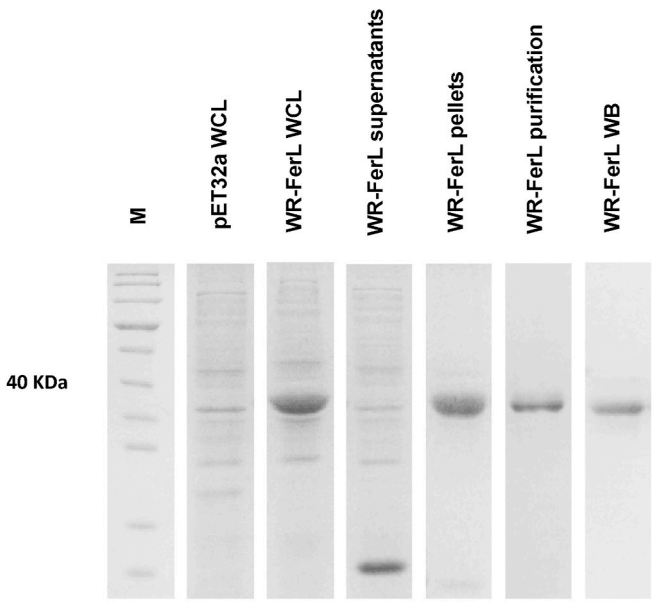

Fig.4A

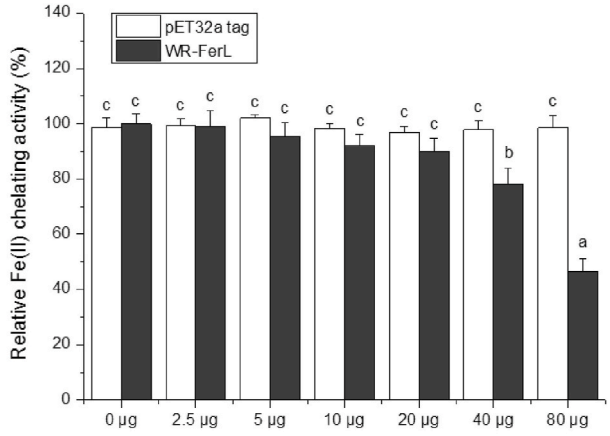

Fig.4B

Fig. 4. WR-FerL fusion protein purification and iron depriving activity. (A) Production and purification of WR-FerL fusion protein. Lane M: Protein molecular standard; Lane pET32a WCL: Total protein was isolated from induced pET32a-Rossetta; Lane WR-FerL WCL: Total protein was isolated from whole cell lysis of induced pET32a-WR-FerL-Rossetta; WR-FerL supernatants: Supernatants from induced pET32a-WR-FerL-Rossetta after sonication; WR-FerL pellets: Pellets from induced pET32a-WR-FerL-Rossetta after sonication; WR-FerL purification: Purified WR-FerL fusion protein; WR-FerL WB: Purified WR-FerL fusion protein was identified using anti-His tag antibody. (B) Iron depriving activity of WR-FerL. The calculated data (mean ± SD) with different letters were significantly different ($P < 0.05$) among the groups. The experiments were performed in triplicate.

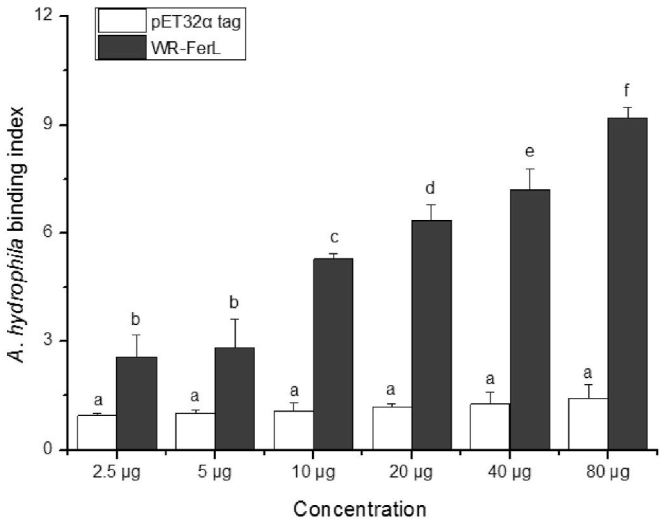

Fig.5A

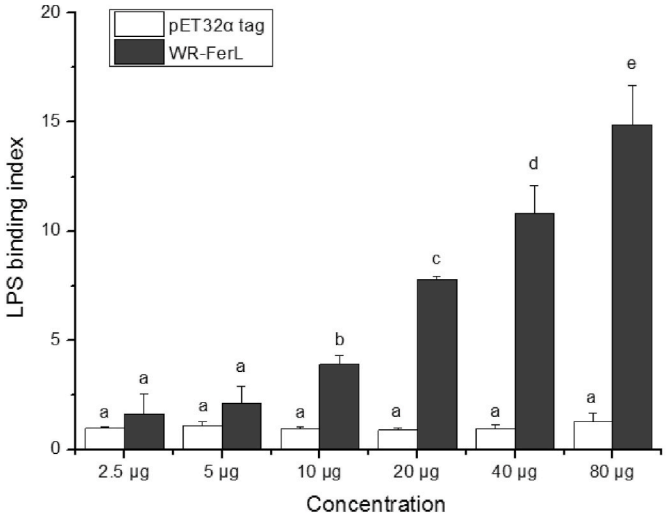

Fig.5B

Fig. 5. Binding activity of WR-FerL to *A. hydrophila* (A) and LPS (B) determined by ELISA assay. The calculated data (mean ± SD) with different letters were significantly different ($P < 0.05$) among the groups. The experiments were performed in triplicate.

and tumor cells, but also plays an important role in the proliferation of immune cells and regulation of cellular immune effectors [66]. As a critical iron-regulatory protein, FerL may play a complex role in immune regulation. In mammals, recent studies indicate that FerL can alleviate LPS-induced productions of inflammatory cytokines [67], ameliorate sepsis-induced organ dysfunction [64] as well as enhance the cellular resistance to temozolomide chemotherapy [68]. However, the mechanism linking FerL to immune regulation in fish is still unclear. To investigate the immune-regulatory function of WR-FerL, WR-FerL protein was generated *in vitro*. ELISA assay indicated that fusion WR-FerL protein could exhibit the *in vitro* binding activity to *A. hydrophila* and LPS in a dose-dependent manner. Then, *in vivo* treatment of WR-FerL revealed that WR-FerL administration could reduce bacterial loads in liver, kidney and spleen. These results suggested that WR-FerL may exert its antibacterial activity by decreasing the adhesion of gram-negative bacteria to cell surface.

A. hydrophila is a gram-negative bacteria, posing a great threat to the survival of economic fish [69]. In general, endotoxin of gram-negative bacteria can directly increase antimicrobial products from ontogeny to adulthood [16] and mediate immune response through toll-like receptors (TLRs) in fish [70]. MyD88 is a pivotal adaptor involved in TLR signals by IRAK4 recruitment [71,72]. IRAK4 activation can promote TRAF6 activation [73,74] and facilitate mRNA stability of cytokines [75], then mediating the induction of proinflammatory cytokines via activation of IκB kinases/nuclear factor-κB (IKKs/NF-κB) and mitogen-activated protein kinase/activator protein-1 (MAPK/AP-1) [76,77]. As is well known, NF-κB is a key transcription factor capable of

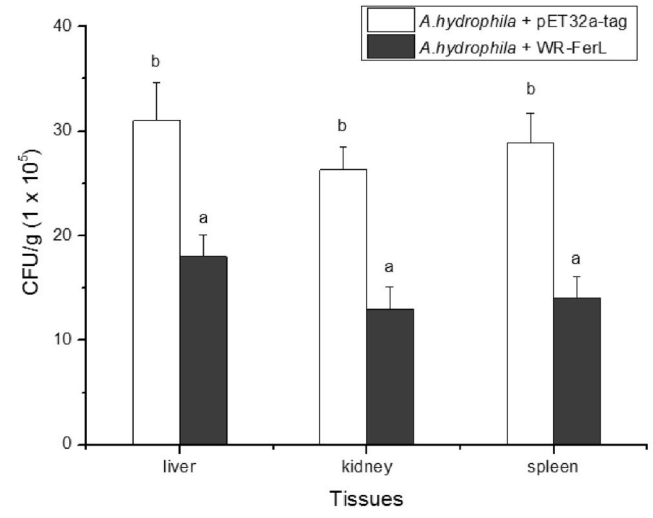

Fig.6A

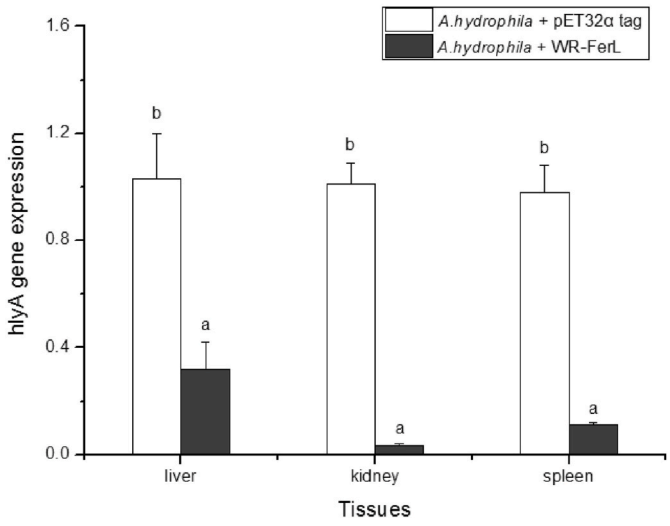

Fig.6B

Fig. 6. Determination of antibacterial activity of WR-FerL. (A) Bacterial load assay. Following injection, liver, kidney and spleen was homogenized in 1 ml of sterile PBS and then cultured in agar medium. (B) Inhibitory effect of WR-FerL on *A. hydrophila* infection *in vivo*. Thirty minutes after *A. hydrophila* infection, treatment of pET32a tag or WR-FerL was performed. Liver, kidney and spleen were isolated at 24 h post-injection. Expression of *A. hydrophila* hlyA gene was determined by qPCR assay. The calculated data (mean ± SD) with different letters were significantly different ($P < 0.05$) among the groups. The experiments were performed in triplicate.

determining the choice between life or death events [78] and participating in cytokine production [79,80]. Thus, to investigate the regulative roles of WR-FerL in *A. hydrophila*-induced inflammation, we performed *A. hydrophila* challenge followed by *in vivo* treatment of above fusion proteins. In this study, gene expressions of MyD88, IRAK4, TRAF6, IL-1β-1, IL-1β-2, TNFα-1 and TNFα-2 were significantly lower in WR-FerL + *A. hydrophila* group by comparing with those of pET32α tag + *A. hydrophila* group. In addition, WR-FerL overexpression could dramatically attenuate NF-κB and TNFα activity in WRFC with or without LPS treatment. Taken together with previous studies, these

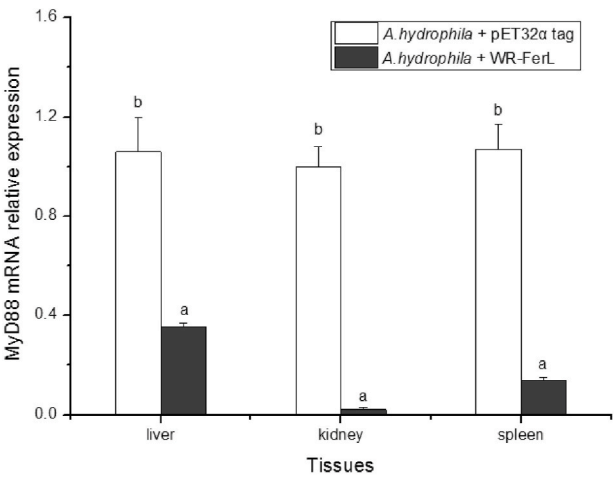

Fig.7A

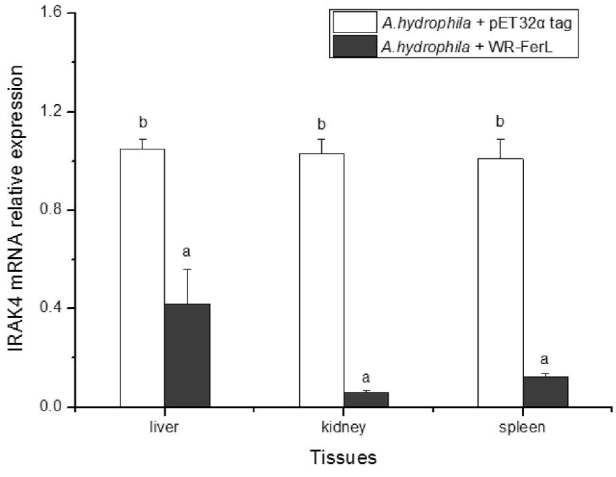

Fig.7B

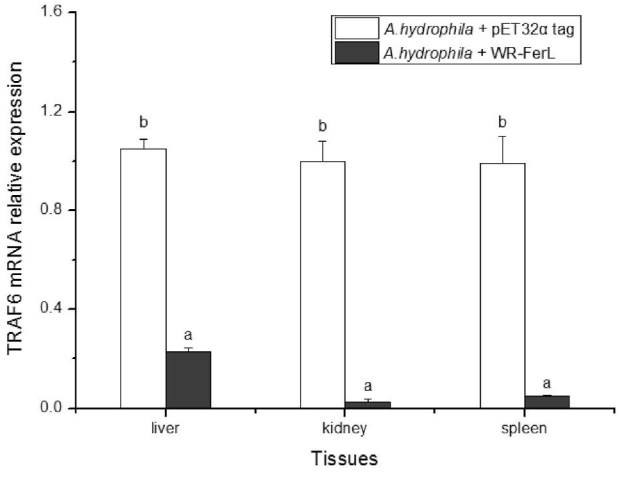

Fig.7C

Fig. 7. Protective effect of WR-FerL in *A. hydrophila*-mediated inflammatory signals. qRT-PCR analysis of MyD88 (A), IRAK4 (B), TRAF6 (C), IL-1β-1 (D), IL-1β-2 (E), TNFα-1 (F) and TNFα-2 (G) mRNA expression in liver, kidney and spleen at 24 h post-challenge. The calculated data (mean ± SD) with different letters were significantly different ($P < 0.05$) among the groups. The experiments were performed in triplicate.

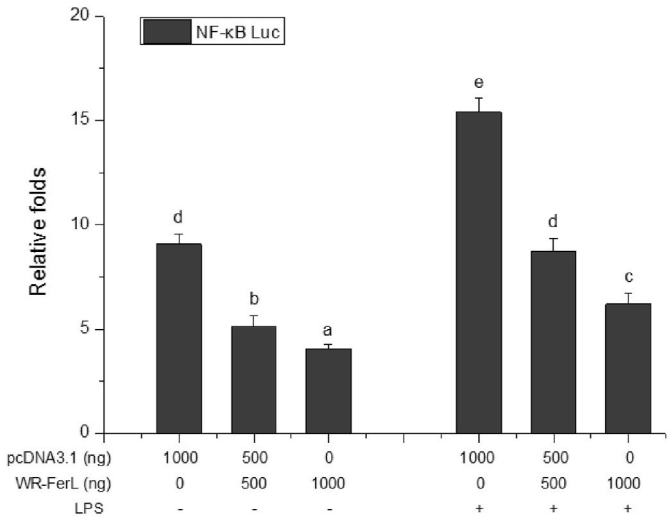

Fig.8A

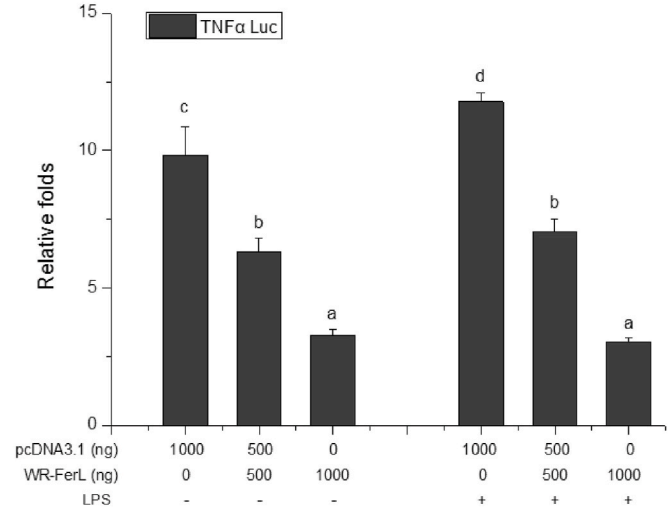

Fig.8B

Fig. 8. Effect of WR-FerL overexpression on the promoter activities. Cells were co-transfected with PRL-TK, NF-κB Luc/TNFα Luc, together with pcDNA3.1 or pcDNA3.1-WR-FerL. The calculated data (mean ± SD) with different letters were significantly different ($P < 0.05$). The experiments were performed in triplicate.

results indicated that WR-FerL may counteract MyD88-IRAK4 proinflammatory signals as well as decrease proinflammatory cytokine productions of IL-1β-1, IL-1β-2, TNFα-1 and TNFα-2 following *A. hydrophila* infection.

In summary, we analyzed the expressions of apoptosis-related genes following *A. hydrophila* challenge. Then, we characterized the architecture of WR-FerL in crucian carp for the first time and studied upregulated expression of WR-FerL mRNA after *A. hydrophila* infection and LPS stimulation. WR-FerL fusion protein could elicit the iron chelating activity, bind to *A. hydrophila* and LPS as well as restrict bacterial dissemination to tissues *in vivo*. In addition, the administration of WR-FerL protein could downregulate bacteria-induced proinflammatory signals and decrease cytokine production. WR-FerL overexpression could alleviate transcript activity of NF-κB and TNFα in WRFCs. Our results revealed that WR-FerL may be involved in the downregulation of inflammatory response in fish following *A. hydrophila* challenge.

Declaration of competing interest

The authors declare that they have no conflict of interest.

Acknowledgements

This research was supported by the National Natural Science Foundation of China, China (grant no. 31902363), Hunan Provincial Natural Science Foundation of China, China (grant no.2021JJ40340) and the Doctoral Publishing Fund of Hunan Normal University, China (grant nos. 0531120-3680).

References

[1] Z. Qi, Y. Zhang, Z.-F. Chen, C. Yang, Y. Song, X. Liao, et al., Chemical identity and cardiovascular toxicity of hydrophobic organic components in PM2. 5, Ecotoxicol. Environ. Saf. 201 (2020), 110827.
[2] Y.Y. Sung, T.H. MacRae, P. Sorgeloos, P. Bossier, Stress response for disease control in aquaculture, Rev. Aquacult. 3 (2011) 120–137.
[3] B. Magnadottir, Immunological control of fish diseases, Mar. Biotechnol. 12 (2010) 361–379.
[4] N.C. Andrews, Disorders of iron metabolism, N. Engl. J. Med. 341 (1999) 1986–1995.
[5] E.E. Johnson, M. Wessling-Resnick, Iron metabolism and the innate immune response to infection, Microb. Infect. 14 (2012) 207–216.
[6] J.M. Fernández-Real, A. López-Bermejo, W. Ricart, Cross-talk between iron metabolism and diabetes, Diabetes 51 (2002) 2348–2354.
[7] I. Majumdar, P. Paul, V. Talib, S. Ranga, The effect of iron therapy on the growth of iron-replete and iron-deplete children, J. Trop. Pediatr. 49 (2003) 84–88.
[8] R. Meneghini, Iron homeostasis, oxidative stress, and DNA damage, Free Radic. Biol. Med. 23 (1997) 783–792.
[9] M. Worwood, Ferritin. *Blood reviews* 4 (1990) 259–269.
[10] R. Scudiero, M.G. Esposito, F. Trinchella, Middle ferritin genes from the icefish Chionodraco rastrospinosus: comparative analysis and evolution of fish ferritins, Comptes Rendus Biol. 336 (2013) 134–141.
[11] K. Robson, Hepcidin and its role in iron absorption, Gut 53 (2004) 617–619.
[12] A.U. Steinbicker, T.B. Bartnikas, L.K. Lohmeyer, P. Leyton, C. Mayeur, S.M. Kao, et al., Perturbation of hepcidin expression by BMP type I receptor deletion induces iron overload in mice, Blood, The Journal of the American Society of Hematology 118 (2011) 4224–4230.
[13] M. Samba-Mondonga, A. Calvé, F.A. Mallette, M.M. Santos, Myd88 regulates the expression of smad4 and the iron regulatory hormone hepcidin, Front. Cell Dev. Biol. 6 (2018) 105.
[14] A. Cuesta, J. Meseguer, M.A. Esteban, The antimicrobial peptide hepcidin exerts an important role in the innate immunity against bacteria in the bony fish gilthead seabream, Mol. Immunol. 45 (2008) 2333–2342.
[15] J.V. Neves, C. Caldas, I. Vieira, M.F. Ramos, P.N. Rodrigues, Multiple hepcidins in a teleost fish, Dicentrarchus labrax: different hepcidins for different roles, J. Immunol. 195 (2015) 2696–2709.
[16] E. Caccia, M. Agnello, M. Ceci, P. Strickler Dinglasan, G.R. Vasta, N. Romano, Antimicrobial peptides are expressed during early development of zebrafish (Danio rerio) and are inducible by immune challenge, Fishes 2 (2017) 20.
[17] Y. Hu, T. Kurobe, X. Liu, Y.-A. Zhang, J. Su, G. Yuan, Hamp type-1 promotes antimicrobial defense via direct microbial killing and regulating iron metabolism in grass carp (Ctenopharyngodon idella), Biomolecules 10 (2020) 825.
[18] Y. Ma, C.-J. Lee, S.-S. Kim, D.N.-J. Kim, B.-H. Nam, Y.-O. Kim, et al., Role of hepcidins from Black Rockfish (Sebastes schlegelii) in iron-metabolic function and bacterial defense, J. Mar. Sci. Eng. 8 (2020) 493.
[19] L. Vanoaica, D. Darshan, L. Richman, K. Schümann, L.C. Kühn, Intestinal ferritin H is required for an accurate control of iron absorption, Cell Metabol. 12 (2010) 273–282.
[20] J.L. Beard, L.E. Murray-Kolb, F.J. Rosales, N.W. Solomons, M.L. Angelilli, Interpretation of serum ferritin concentrations as indicators of total-body iron stores in survey populations: the role of biomarkers for the acute phase response, Am. J. Clin. Nutr. 84 (2006) 1498–1505.
[21] D.S.T. Ong, L. Wang, Y. Zhu, B. Ho, J. Ding, The response of ferritin to LPS and acute phase of Pseudomonas infection, J. Endotoxin Res. 11 (2005) 267–280.
[22] G. Zandman-Goddard, Y. Shoenfeld, Ferritin in autoimmune diseases, Autoimmun. Rev. 6 (2007) 457–463.
[23] M.C.H. Holland, J.D. Lambris, The complement system in teleosts, Fish Shellfish Immunol. 12 (2002) 399–420.
[24] J.B. Jørgensen, The innate immune response in fish, Fish vaccination 1 (2014) 84–102.
[25] Z. Ding, X. Zhao, Q. Zhan, L. Cui, Q. Sun, W. Wang, et al., Comparative analysis of two ferritin subunits from blunt snout bream (Megalobrama amblycephala): characterization, expression, iron depriving and bacteriostatic activity, Fish Shellfish Immunol. 66 (2017) 411–422.

[26] O. Andersen, A. Dehli, H. Standal, T. Giskegjerde, R. Karstensen, K. Rørvik, Two ferritin subunits of Atlantic salmon (Salmo salar): cloning of the liver cDNAs and antibody preparation, Mol. Mar. Biol. Biotechnol. 4 (1995) 164–170.
[27] H. Liu, T. Takano, E. Peatman, J. Abernathy, S. Wang, Z. Sha, et al., Molecular characterization and gene expression of the channel catfish ferritin H subunit after bacterial infection and iron treatment, J. Exp. Zool. Part A: Ecological Genetics and Physiology 313 (2010) 359–368.
[28] X. Zhang, W. Wei, H. Wu, H. Xu, K. Chang, Y. Zhang, Gene cloning and characterization of ferritin H and M subunits from large yellow croaker (Pseudosciaena crocea), Fish Shellfish Immunol. 28 (2010) 735–742.
[29] M. Oh, N. Umasuthan, D.A.S. Elvitigala, Q. Wan, E. Jo, J. Ko, et al., First comparative characterization of three distinct ferritin subunits from a teleost: evidence for immune-responsive mRNA expression and iron depriving activity of seahorse (Hippocampus abdominalis) ferritins, Fish Shellfish Immunol. 49 (2016) 450–460.
[30] Z. Li, Z.W. Wang, Y. Wang, J.F. Gui, Crucian Carp and Gibel Carp Culture. *Aquaculture in China: Success Stories and Modern Trends*, 2018, pp. 149–157.
[31] J. Luo, Y. Gao, W. Ma, X. Bi, S. Wang, J. Wang, et al., Tempo and mode of recurrent polyploidization in the Carassius auratus species complex (Cypriniformes, Cyprinidae), Heredity 112 (2014) 415–427.
[32] Q. Liu, J. Liu, Q. Liang, Y. Qi, M. Tao, C. Zhang, et al., A hybrid lineage derived from hybridization of Carassius cuvieri and Carassius auratus red var. and a new type of improved fish obtained by back-crossing, Aquaculture 505 (2019) 173–182.
[33] G. Choo, H.-S. Cho, K. Park, J.-W. Lee, P. Kim, J.-E. Oh, Tissue-specific distribution and bioaccumulation potential of organophosphate flame retardants in crucian carp, Environ. Pollut. 239 (2018) 161–168.
[34] T.J. Bowden, Modulation of the immune system of fish by their environment, Fish Shellfish Immunol. 25 (2008) 373–383.
[35] D. Marcogliese, The impact of climate change on the parasites and infectious diseases of aquatic animals, Rev Sci Tech 27 (2008) 467–484.
[36] B. Liu, L. Xu, X. Ge, J. Xie, P. Xu, Q. Zhou, et al., Effects of mannan oligosaccharide on the physiological responses, HSP70 gene expression and disease resistance of Allogynogenetic crucian carp (Carassius auratus gibelio) under Aeromonas hydrophila infection, Fish Shellfish Immunol. 34 (2013) 1395–1403.
[37] Q. Liu, Y. Qi, Q. Liang, X. Xu, F. Hu, J. Wang, et al., The chimeric genes in the hybrid lineage of Carassius auratus cuvieri (♀)× Carassius auratus red var.(♂), Sci. China Life Sci. 61 (2018) 1079–1089.
[38] S.-W. Luo, Z.-W. Mao, Z.-Y. Luo, N.-X. Xiong, K.-K. Luo, S.-J. Liu, et al., Chimeric ferritin H in hybrid crucian carp exhibit a similar down-regulation in lipopolysaccharide-induced NF-κB inflammatory signal in comparison with Carassius cuvieri and Carassius auratus red var, Comp. Biochem. Physiol. C Toxicol. Pharmacol. (2021), 108966.
[39] C.-H. Cheng, F.-F. Yang, S.-A. Liao, Y.-T. Miao, C.-X. Ye, A.-L. Wang, Effect of acute ammonia exposure on expression of GH/IGF axis genes GHR1, GHR2 and IGF-1 in pufferfish (Takifugu obscurus), Fish Physiol. Biochem. 41 (2015) 495–507.
[40] S.-W. Luo, K.-K. Luo, S.-J. Liu, ITLN in diploid hybrid fish (Carassius auratus cuvieri♀× Carassius auratus red var♂) is involved in host defense against bacterial infection, Dev. Comp. Immunol. 103 (2020), 103520.
[41] H. Van Doan, S. Doolgindachabaporn, A. Suksri, The LD50 of Asian Catfish (Pangasius bocourti, Sauvage 1870) challenge to pathogen Aeromonas hydrophila FW52 strain, Pensee (2013) 75.
[42] C. Fierro-Castro, L. Barrioluengo, P. López-Fierro, B. Razquin, A. Villena, Fish cell cultures as in vitro models of inflammatory responses elicited by immunostimulants. Expression of regulatory genes of the innate immune response, Fish Shellfish Immunol. 35 (2013) 979–987.
[43] N.-X. Xiong, S.-W. Luo, L.-F. Fan, Z.-W. Mao, K.-K. Luo, S.-J. Liu, et al., Comparative analysis of erythrocyte hemolysis, plasma parameters and metabolic features in red crucian carp (Carassius auratus red var) and triploid hybrid fish following Aeromonas hydrophila challenge, Fish Shellfish Immunol. 118 (2021) 369–384.
[44] Y. Yang, H. Yu, H. Li, A. Wang, Transcriptome profiling of grass carp (Ctenopharyngodon idellus) infected with Aeromonas hydrophila, Fish Shellfish Immunol. 51 (2016) 329–336.
[45] K.J. Livak, T.D. Schmittgen, Analysis of relative gene expression data using real-time quantitative PCR and the 2− ΔΔCT method, Methods 25 (2001) 402–408.
[46] C.-H. Cheng, F.-F. Yang, S.-A. Liao, Y.-T. Miao, C.-X. Ye, A.-L. Wang, et al., Identification, characterization and functional analysis of anti-apoptotic protein BCL-2-like gene from pufferfish, Takifugu obscurus, responding to bacterial challenge, Fish Physiol. Biochem. 41 (2015) 1053–1064.
[47] Z-h Qi, Y-f Liu, W-n Wang, Y. Xin, F-x Xie, A.-L. Wang, Fatty acid binding protein 10 in the orange-spotted grouper (Epinephelus coioides): characterization and regulation under pH and temperature stress, Comp. Biochem. Physiol. C Toxicol. Pharmacol. 155 (2012) 447–455.
[48] N.-X. Xiong, S.-W. Luo, Z.-W. Mao, L.-F. Fan, K.-K. Luo, S. Wang, et al., Ferritin H can counteract inflammatory response in hybrid fish and its parental species after Aeromonas hydrophila infection, Comp. Biochem. Physiol. C Toxicol. Pharmacol. (2021), 109174.
[49] M. De Zoysa, J. Lee, Two ferritin subunits from disk abalone (Haliotis discus discus): cloning, characterization and expression analysis, Fish Shellfish Immunol. 23 (2007) 624–635.
[50] J.S. Plested, P.A. Coull, M.A.J. Gidney, Elisa, Haemophilus influenzae Protocols (2003) 243–261.
[51] L. Wang, C. Fan, W. Xu, Y. Zhang, Z. Dong, J. Xiang, et al., Characterization and functional analysis of a novel C1q-domain-containing protein in Japanese flounder (Paralichthys olivaceus), Dev. Comp. Immunol. 67 (2017) 322–332.
[52] H.-X. Li, X.-J. Lu, C.-H. Li, J. Chen, Molecular characterization of the liver-expressed antimicrobial peptide 2 (LEAP-2) in a teleost fish, Plecoglossus altivelis: antimicrobial activity and molecular mechanism, Mol. Immunol. 65 (2015) 406–415.
[53] C. Yang, L. Liu, J. Liu, Z. Ye, H. Wu, P. Feng, et al., Black carp IRF5 interacts with TBK1 to trigger cell death following viral infection, Dev. Comp. Immunol. 100 (2019), 103426.
[54] S.-W. Luo, N.-X. Xiong, Z.-Y. Luo, K.-K. Luo, S.-J. Liu, C. Wu, et al., Effect of Lipopolysaccharide (LPS) stimulation on apoptotic process and oxidative stress in fibroblast cell of hybrid crucian carp compared with those of Carassius cuvieri and Carassius auratus red var, Comp. Biochem. Physiol. C Toxicol. Pharmacol. 248 (2021), 109085.
[55] E. Odkhuu, A. Mendjargal, N. Koide, Y. Naiki, T. Komatsu, T. Yokochi, Lipopolysaccharide downregulates the expression of p53 through activation of MDM2 and enhances activation of nuclear factor-kappa B, Immunobiology 220 (2015) 136–141.
[56] Y.J. Suzuki, H.J. Forman, A. Sevanian, Oxidants as stimulators of signal transduction, Free Radic. Biol. Med. 22 (1997) 269–285.
[57] K.J. Davies, Oxidative stress, antioxidant defenses, and damage removal, repair, and replacement systems, IUBMB Life 50 (2000) 279–289.
[58] J. Savill, Apoptosis in resolution of inflammation, J. Leukoc. Biol. 61 (1997) 375–380.
[59] E.E. McGrath, H.M. Marriott, A. Lawrie, S.E. Francis, I. Sabroe, S.A. Renshaw, et al., TNF-related apoptosis-inducing ligand (TRAIL) regulates inflammatory neutrophil apoptosis and enhances resolution of inflammation, J. Leukoc. Biol. 90 (2011) 855–865.
[60] J. Reed, Balancing cell life and death: bax, apoptosis, and breast cancer, J. Clin. Invest. 97 (1996) 2403.
[61] Y. Deng, Y. Lin, X. Wu, TRAIL-induced apoptosis requires Bax-dependent mitochondrial release of Smac/DIABLO, Genes Dev. 16 (2002) 33–45.
[62] S.P. Cregan, J.G. MacLaurin, C.G. Craig, G.S. Robertson, D.W. Nicholson, D.S. Park, et al., Bax-dependent caspase-3 activation is a key determinant in p53-induced apoptosis in neurons, J. Neurosci. 19 (1999) 7860–7869.
[63] S. Hao, Y. Zhang, L. Hua, N. Xie, N. Xiao, H. Wang, et al., Antibodies specific to ferritin light chain polypeptide are frequently detected in patients with immune-related pancytopenia, Mol. Med. Rep. 22 (2020) 2012–2020.
[64] A. Zarjou, L.M. Black, K.R. McCullough, T.D. Hull, S.K. Esman, R. Boddu, et al., Ferritin light chain confers protection against sepsis-induced inflammation and organ injury, Front. Immunol. 10 (2019) 131.
[65] C.M. Press, Ø. Evensen, The morphology of the immune system in teleost fishes, Fish Shellfish Immunol. 9 (1999) 309–318.
[66] G. Weiss, H. Wachter, D. Fuchs, Linkage of cell-mediated immunity to iron metabolism, Immunol. today 16 (1995) 495–500.
[67] Y. Fan, J. Zhang, L. Cai, S. Wang, C. Liu, Y. Zhang, et al., The effect of anti-inflammatory properties of ferritin light chain on lipopolysaccharide-induced inflammatory response in murine macrophages, Biochim. Biophys. Acta Mol. Cell Res. 1843 (2014) 2775–2783.
[68] J. Liu, L. Gao, N. Zhan, P. Xu, Y. Xu, Q. Cai, et al., Hypoxia induced ferritin light chain (FTL) promoted epithelia mesenchymal transition and chemoresistance of glioma, J. Exp. Clin. Cancer Res. 39 (2020) 1–17.
[69] C.J. Gonzalez-Serrano, J.A. Santos, M.L. Garcia-Lopez, A. Otero, Virulence markers in Aeromonas hydrophila and Aeromonas veronii biovar sobria isolates from freshwater fish and from a diarrhoea case, J. Appl. Microbiol. 93 (2010) 414–419.
[70] T. Xu, Y. Wang, J. Li, C. Shu, J. Han, Q. Chu, Comparative genomic evidence for duplication of TLR1 subfamily and miiuy croaker TLR1 perceives LPS stimulation via MyD88 and TIRAP, Fish Shellfish Immunol. 56 (2016) 336–348.
[71] H. Wesche, W.J. Henzel, W. Shillinglaw, S. Li, Z. Cao, MyD88: an adapter that recruits IRAK to the IL-1 receptor complex, Immunity 7 (1997) 837–847.
[72] T. Kawai, O. Adachi, T. Ogawa, K. Takeda, S. Akira, Unresponsiveness of MyD88-deficient mice to endotoxin, Immunity 11 (1999) 115–122.
[73] E. Lye, C. Mirtsos, N. Suzuki, S. Suzuki, W.-C. Yeh, The role of interleukin 1 receptor-associated kinase-4 (IRAK-4) kinase activity in IRAK-4-mediated signaling, J. Biol. Chem. 279 (2004) 40653–40658.
[74] H. Ye, J.R. Arron, B. Lamothe, M. Cirilli, T. Kobayashi, N.K. Shevde, et al., Distinct molecular mechanism for initiating TRAF6 signalling, Nature 418 (2002) 443–447.
[75] T.W. Kim, K. Staschke, K. Bulek, J. Yao, K. Peters, K.-H. Oh, et al., A critical role for IRAK4 kinase activity in Toll-like receptor–mediated innate immunity, J. Exp. Med. 204 (2007) 1025–1036.
[76] J. Gohda, T. Matsumura, J-i Inoue, Cutting edge: TNFR-associated factor (TRAF) 6 is essential for MyD88-dependent pathway but not Toll/IL-1 receptor domain-containing adaptor-inducing IFN-β (TRIF)-dependent pathway in TLR signaling, J. Immunol. 173 (2004) 2913–2917.
[77] L. Chang, M. Karin, Mammalian MAP kinase signalling cascades, Nature 410 (2001) 37–40.
[78] M. Karin, A. Lin, NF-κB at the crossroads of life and death, Nat. Immunol. 3 (2002) 221–227.
[79] C.J. Hunter, I.G. De Plaen, Inflammatory signaling in NEC: role of NFKB and cytokines, Pathophysiology: the official journal of the International Society for Pathophysiology/ISP 21 (2014) 55.
[80] F. Diomede, M. Zingariello, M.F. Cavalcanti, I. Merciaro, J. Pizzicannella, N. de Isla, et al., MyD88/ERK/NFkB pathways and pro-inflammatory cytokines release in periodontal ligament stem cells stimulated by Porphyromonas gingivalis, Eur. J. Histochem.: EJH (2017) 61.